

Electronic Supporting Information (ESI)

Highly efficient phosphorescent OLEDs with host-independent and concentration-insensitive properties based on a bipolar iridium complex

Tai Peng,[†] Guomeng Li,[†] Kaiqi Ye,[†] Chenguang Wang,[†] Shanshan Zhao,[†] Yu Liu,^{†*}
Zhaomin Hou,[‡] and Yue Wang^{†*}

[†]State Key Laboratory of Supramolecular Structure and Materials, Jilin University, Changchun 130012, People's Republic of China.

E-mail: (Y L: yuliu@jlu.edu.cn and Y W: yuewang@jlu.edu.cn)

[‡]Organometallic Chemistry Laboratory, RIKEN Advanced Science Institute, 2-1 Hirosawa, Wako, Saitama 351-0198, Japan.

Single-Crystal XRD Data of Crystals: Single crystals suitable for X-ray structural analysis were obtained by vacuum sublimation. Diffraction data were collected on a Rigaku R-Axis Rapid diffractometer (Mo K α radiation, graphite monochromator) in the ψ rotation scan mode. The structure determination was performed by direct methods using SHELXTL 5.01v and refinements with full-matrix least squares on F^2 .

The crystal packing diagram of (ppy)₂Ir(dipig) was given in **Fig. 2a**, and **Fig. S1** is not a packing diagram. The corresponding CCDC reference number is 808967. The data can be obtained free of charge from The Cambridge Crystallographic Data Centre via www.ccdc.cam.ac.uk/data_request/cif.

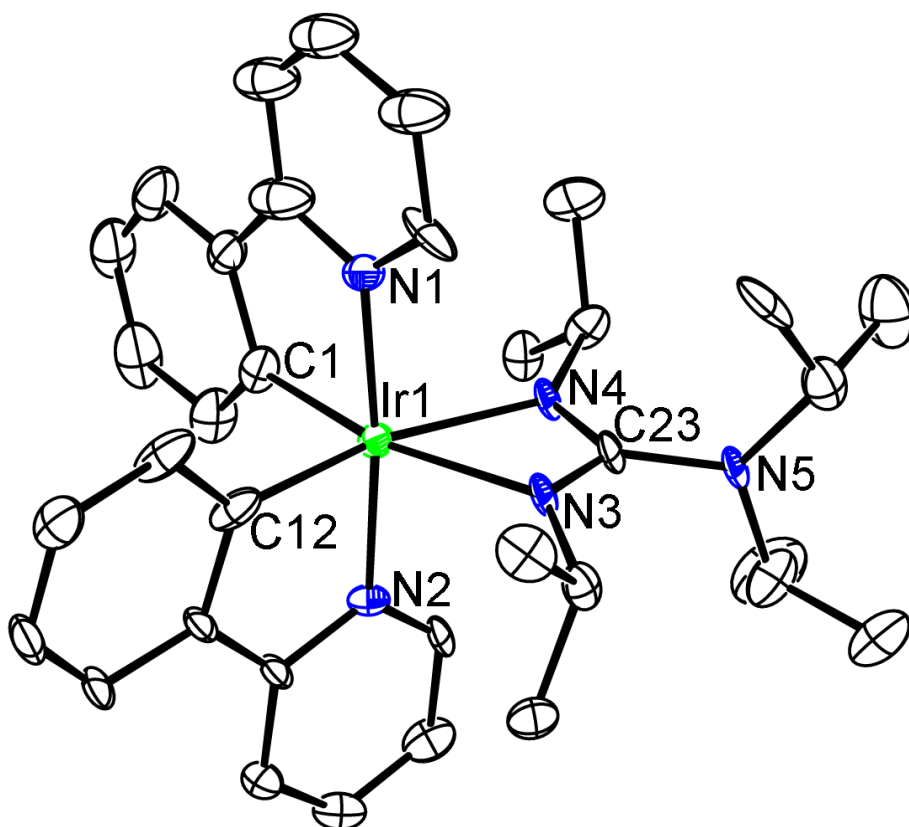


Fig. S1 ORTEP drawing of $[(ppy)_2Ir(dipig)]$ with thermal ellipsoids at 30 % probability. Hydrogen atoms have been omitted for clarity. Selected bond lengths (Å) and angles (°): Ir1-C1 2.014(11), Ir1-C12 2.000(12), Ir1-N1 2.043(9), Ir1-N2 2.024(8), Ir1-N3 2.197(8), Ir1-N4 2.175(8), C(1)-Ir(1)-N(1) 80.8(5), C(1)-Ir(1)-N(3) 164.6(4), C(1)-Ir(1)-N(4) 105.7(4), C(12)-Ir(1)-C(1) 87.7(5), C(12)-Ir(1)-N(2) 81.0(4), C(12)-Ir(1)-N(3) 107.7(4), N(2)-Ir(1)-N(1) 174.0(3), N(3)-Ir(1)-N(4) 59.1(3).

The molecular structure of $(ppy)_2Ir(dipig)$ was determined by X-ray analysis as shown in **Fig. S1**. The iridium metal center is bonded to two bidentate ppy ligands and one chelating guanidinate ligand in a distorted octahedral fashion. The coordination geometry of the $(ppy)_2Ir$ fragment in $(ppy)_2Ir(dipig)$ is similar to those in $[Ir(ppy)_2(acac)]$ (acac = acetoacetate)^{2b} and $[(ppy)_2Ir(dipba)]$ (dipba = *N,N'*-diisopropyl benzamidinate),^{13a} in which the *cis*-C,C- and *trans*-N,N-configuration is retained. The bond lengths of the Ir-C bonds (av. 2.01(1) Å) and the Ir-N(ppy) bonds (av. 2.03(1) Å) in $(ppy)_2Ir(dipig)$ are comparable with those in $[Ir(ppy)_2(acac)]$ (Ir-C: av 2.003(9) Å, Ir-N: 2.010(9) Å)^{2b} and $[(ppy)_2Ir(dipba)]$ (Ir-C: av. 2.01 Å, Ir-N: av. 2.04 Å),^{13a} respectively. The bond lengths of the Ir-N(guanidinate) bonds (av. 2.19 Å) in $(ppy)_2Ir(dipig)$ are longer than those of the Ir-N(ppy) bonds, but are similar to those of the Ir-N(amidinate) bonds (av. 2.18 Å) in $[(ppy)_2Ir(dipba)]$.^{13a}

Time-Of-Flight (TOF) Measurement: The time-of-flight (TOF) technique involves generation of carriers near one electrode with a short pulse of light and observation of the current displaced in the external circuit by the motion of the carriers through the sample. The sample for TOF measurement has been prepared on the glass substrate covered with indium tin oxide (ITO) layer with the structure of [(ITO)/(ppy)₂Ir(dipig) (1 μm)/Al]. An intense short duration (5-6 ns) light pulse from a frequency-tripled (355 nm) Nd:YAG laser was incident at one side of the sample to generate photocarriers. The sample was mounted in a vacuum and measurement was made at the electric field of $5.0 \times 10^5 \text{ V cm}^{-1}$ under room temperature (293 K) (see Fig. S2).

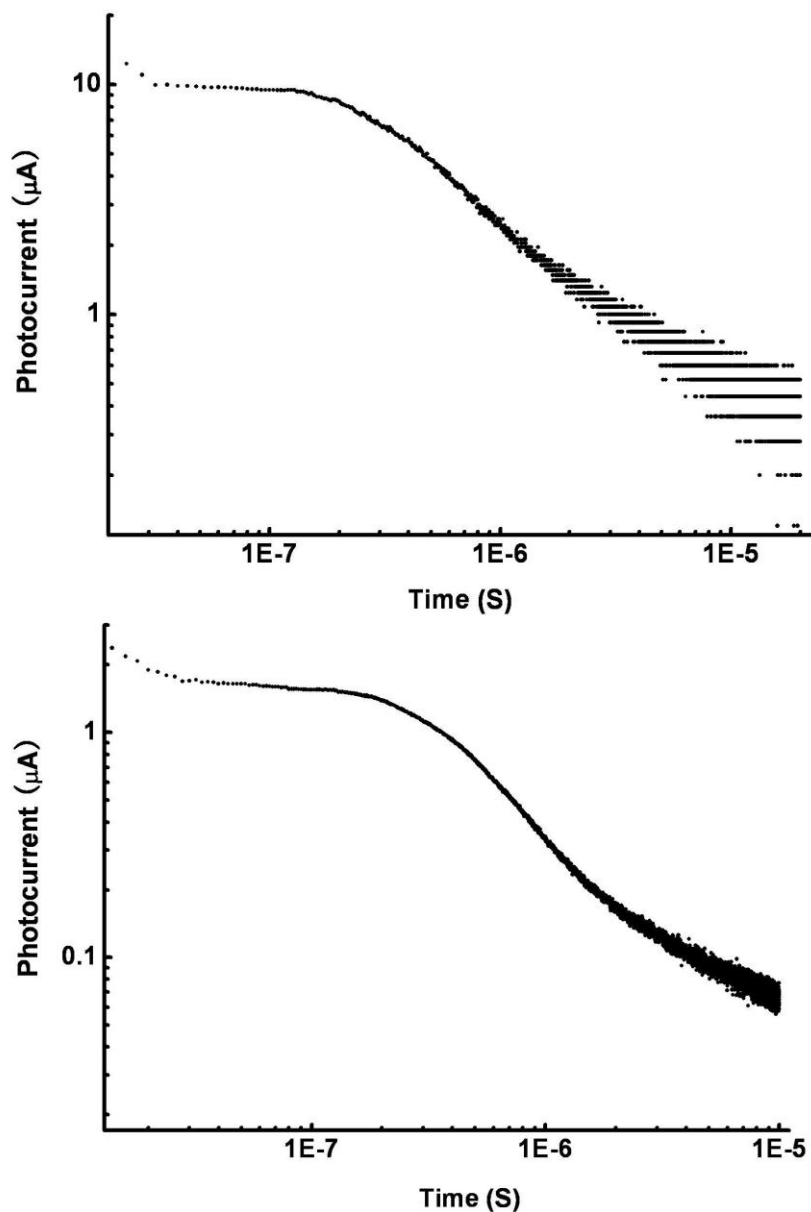


Fig. S2 Log of the photocurrent vs. the log of time in a time-of-flight measurement of hole mobility (top) and electron mobility (bottom) in a 1 μm (ppy)₂Ir(dipig) film at ambient temperature and an electric field of $5.0 \times 10^5 \text{ V cm}^{-1}$.

Single-Carrier Measurement: Single-carrier devices were fabricated using the following configurations: [ITO/TPBI (10 nm)/active molecular layer (80 nm)/LiF/Al] (electron-only device) and [ITO/active molecular layer (80 nm)/MoO₃ (10 nm)/Al] (hole-only device). For comparison purpose, neat NPB and 15 wt % (ppy)₂Ir(dipig) doped in NPB, neat TPBI and 15 wt % (ppy)₂Ir(dipig) doped in TPBI were used as the active molecular layers for electron-only and hole-only devices, respectively (see Fig. S3).

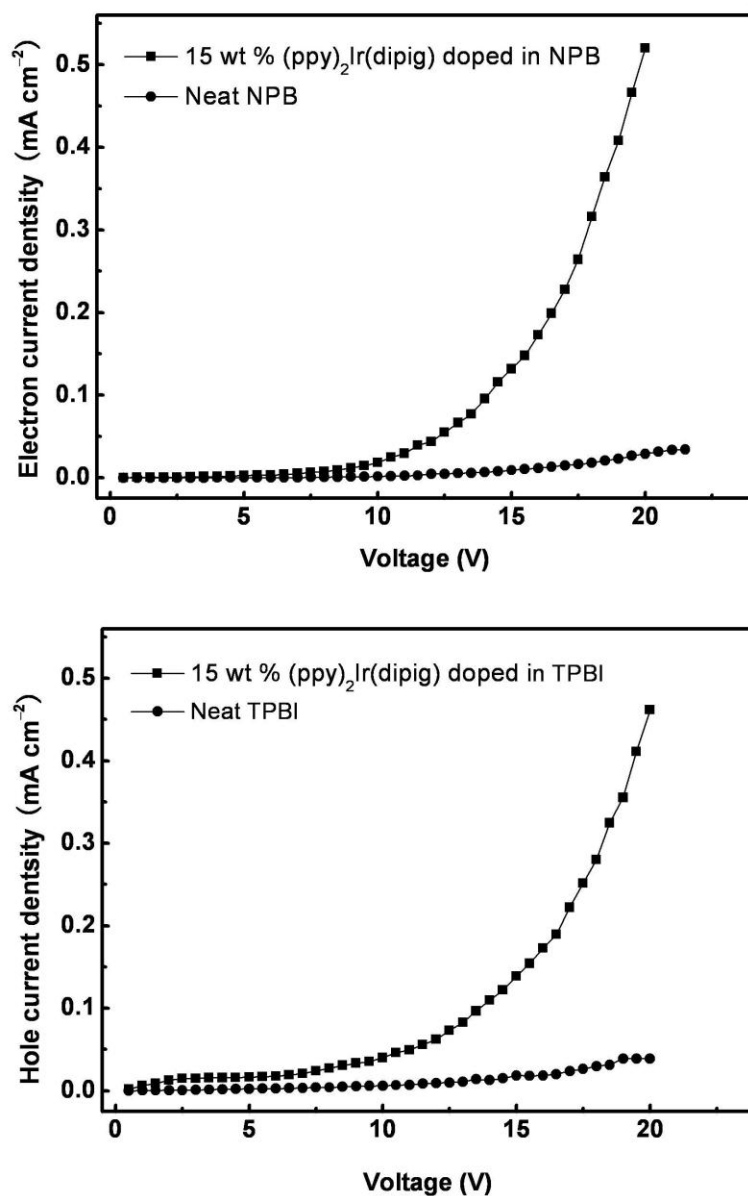


Fig. S3 Current density-electric field characteristics of the electron-only devices: ITO/TPBI/ neat NPB or 15 wt % (ppy)₂Ir(dipig) doped in NPB/LiF/Al (top), and the hole-only devices: ITO/neat TPBI or 15 wt % (ppy)₂Ir(dipig) doped in TPBI/MoO₃/Al (bottom).

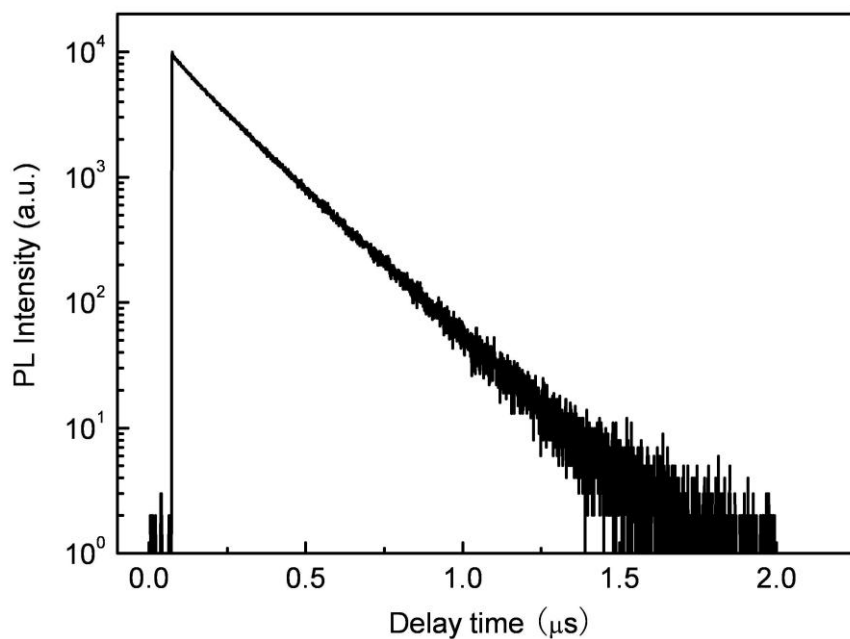


Fig. S4 Transient photoluminescence decay of $(ppy)_2Ir(dipig)$.

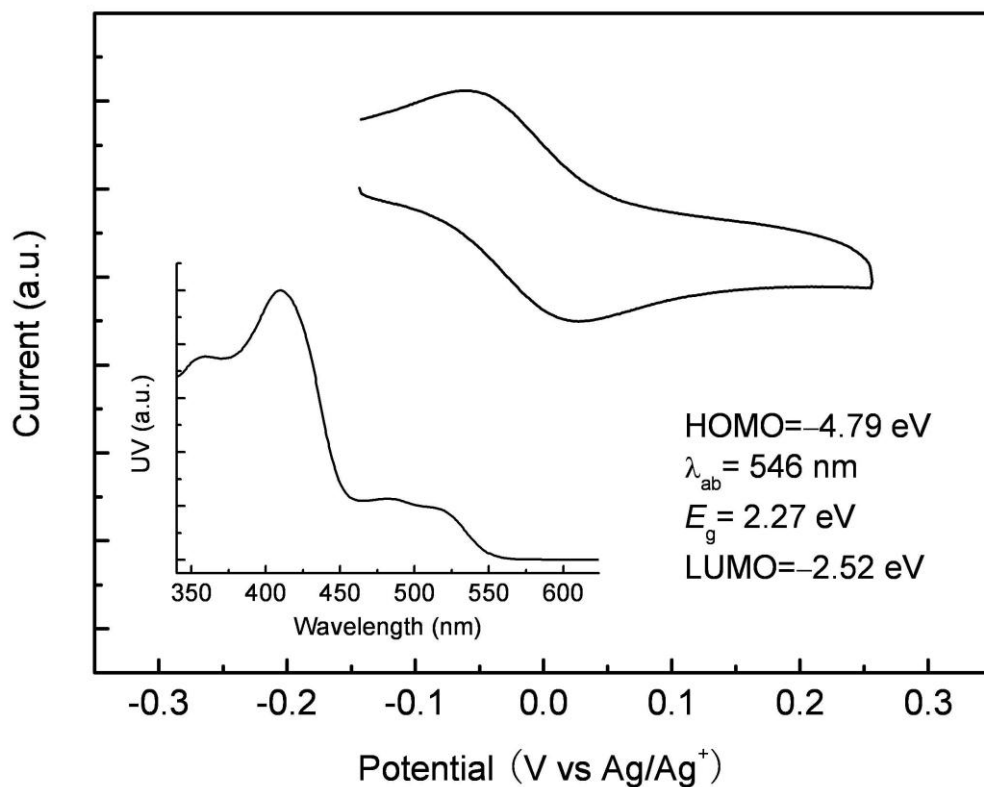


Fig. S5 Cyclic Voltammetry (CV) diagram of $(ppy)_2Ir(dipig)$ in dichloromethane. Inset shows the UV-vis absorption spectrum of $(ppy)_2Ir(dipig)$ in dichloromethane.

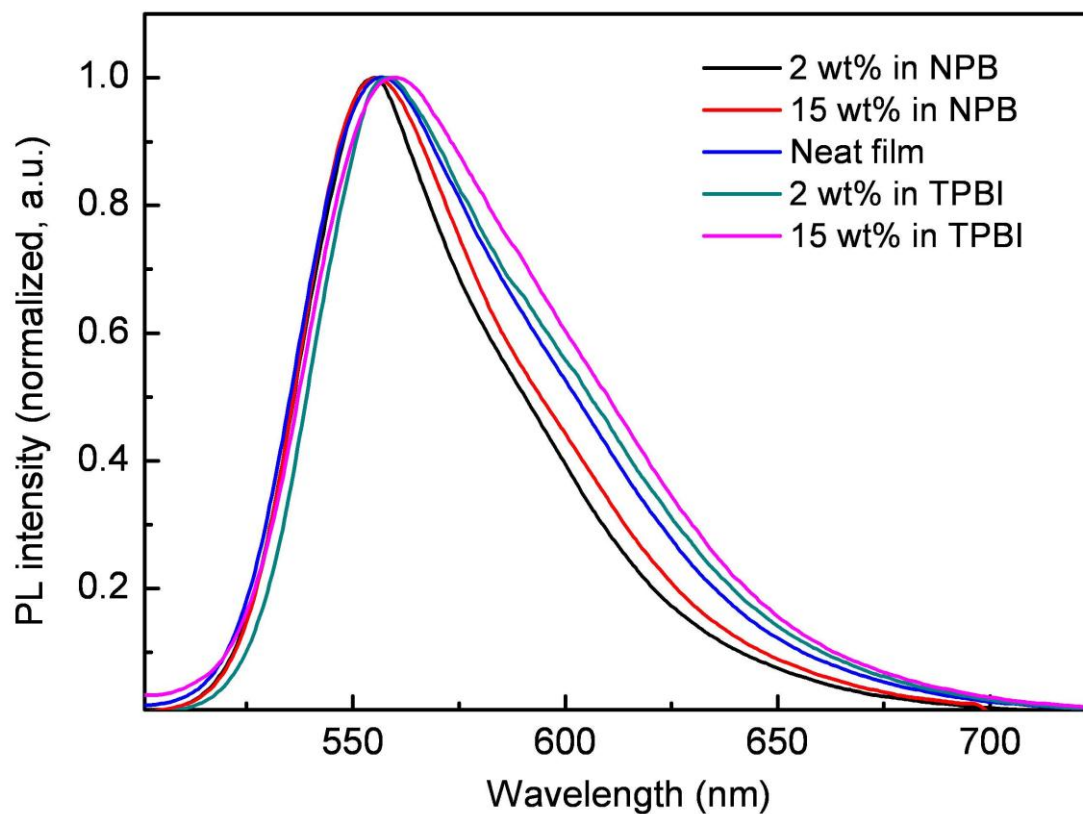


Fig. S6 Photoluminescence (PL) spectra of (ppy)₂Ir(dipig) doped in NPB (2 wt% and 15 wt%) thin films with the quantum yield of 0.95 ± 0.03 and 0.38 ± 0.03 , respectively, PL spectra of (ppy)₂Ir(dipig) in neat thin film with the quantum yield of 0.11 ± 0.01 , and (PL) spectra of (ppy)₂Ir(dipig) doped in TPBI (2 wt% and 15 wt%) thin films with the quantum yield of 0.92 ± 0.03 and 0.63 ± 0.03 , respectively.